Molecular Condensate in a Membrane: A Tugging Game Between Hydrophobicity and Polarity with Its Biological Significance

Shasha Feng^{1†}, Lingyang Kong^{2†}, Stephen Gee^{2†}, Wonpil Im^{1,2,3*}

¹Departments of Biological Sciences, Lehigh University, Bethlehem, Pennsylvania 18015, USA

²Department of Bioengineering, Lehigh University, Bethlehem, Pennsylvania 18015, USA

³Departments of Chemistry, Lehigh University, Bethlehem, Pennsylvania 18015, USA

[†]These authors contributed equally to this work.

^{*}Corresponding authors: wonpil@lehigh.edu, phone (610) 758-4524.

ABSTRACT

Lipid self-organization and lipid-water interfaces have been an increasingly important topic positioned at the crossroad of physical chemistry and biology. Some neutral lipids can partition into the biomembrane and play an important biological role. In this study, we have used all-atom molecular dynamics to dissect the partition, aggregation, flip-flop, and modulation of neutral lipids including i) menaquinone/menaquinol, ii) ubiquinone/ubiquinol, and iii) triacylglycerol. The partition of these molecules is driven by the balancing force between headgroup hydrophilicity and acyl chain hydrophobicity, as well as the lipid shapes. We then discuss the emerging questions in this area, share our own perspectives, and mention the development of the CHARMM-GUI membrane modeling platform, which enables further computational investigations into those questions.

Keywords: molecular dynamics simulation, neutral lipid, non-bilayer lipid, ubiquinone, menaquinone, triacylglyceride, phase segregation, membrane partition, drug partition

1. Introduction

Phospholipids are amphiphilic molecules that can pack to form bilayers and multilamellar layers. Their bilayer-forming properties lay the basis of life that uses the membrane matrix to define cell boundaries and anchor bio-machineries and signaling pathways. Considerable efforts have been devoted to study the lipid self-organization process and lipid-water interface, which form the foundation for membrane dynamics for lipid raft disruption, lipid droplet formation, drug sequestration, as well as membrane protein functions.

A special component in biomembranes are neutral lipids, which have received increasing attention. Neutral lipids can partition into the membranes with examples including cholesterol, diacylglyceride, triacylglyceride, monogalactosyldiacylglycerol, quinones, and squalene.³ They are also called non-bilayer-forming lipids, because they are unable to assemble into a pure bilayer by themselves. Non-bilayer-forming lipids also include lipids like phosphatidylethanolamine and arachidonic acid, which, due to their conical shape, have a negative membrane curvature and therefore cannot assemble into a pure bilayer.

Neutral lipids play important roles in biology. For example, ubiquinone shuttles electrons for the respiratory chain in the mitochondria, menaquinone is important for osmotic pressure resistance in archaea, and triacylglyceride stores energy for animals. Because of their non-bilayer-forming property, neutral lipids pose a unique challenge to experimental characterizations. Studies have indicated that 'fluid lamellar phases' exist for squalane in the archaea-mimicking membrane. ⁴ Triacylglycerol blisters in the bilayer have long been proposed based on ¹H-NMR measurement, optical microscope, and thin-layer chromatography results. ⁵ However, the detailed molecular partition, membrane micro-structure, and modulation exerted by these molecules require more thorough investigations.

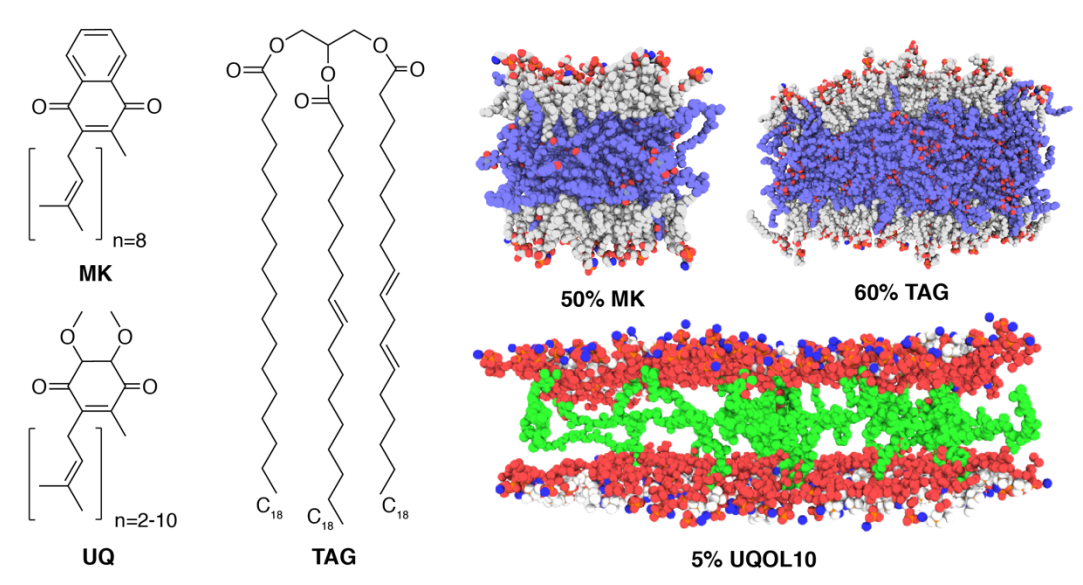


Figure 1. Molecular structures and simulation system snapshots of menaquinone (MK), ubiquinone (UQ), and triacylglycerol (TAG) molecules. The oxygen atoms are red, acyl chain of phospholipids are white, MK tails and TAG tails are purple, and ubiquinol (UQOL) tails are green.

Over the past decade, molecular dynamics (MD) simulation has become an essential tool to study membrane properties. This is largely due to the improvement of force field parameters, availability

of membrane building protocols and software, as well as the growing power of high-performance computers. There are several reviews⁶⁻⁹ for membrane MD simulations. In this Perspective, we show the structure and properties of neutral lipid-containing membranes using all-atom MD simulations of three examples, i.e., menaquinone, ubiquinone, and triacylglycerol (**Figure 1**). Then, the membrane structures containing these three molecules are dissected and analyzed. Finally, we discuss the emerging questions in this area with the insights gained from these simulations, share our own perspectives, and mention the development of the CHARMM-GUI membrane modeling platform, which enables further computational investigations into those questions.

2. Menaquinone condensate in a halobacterial membrane

Menaquinone (MK), also known as vitamin K2, is an isoprenoid compound. In humans, it contributes to bone and cardiovascular health; ¹⁰ in halobacteria, it has been hypothesized to carry electrons and contribute to hyper-osmotic pressure resistance. MK molecules were reported to be up to 48% of the membrane of *Halo. sodomense* from whole-cell measurements. ¹¹ This is an extremely high amount, given the fact that a similar analogue, ubiquinone, is available in mitochondria and bacterial membranes at a concentration of 1-5%. ^{12, 13} MK has a naphthalene ring, connected with a typical isoprenyl group, which can vary from 2-8 in biological systems (**Figure 1**).

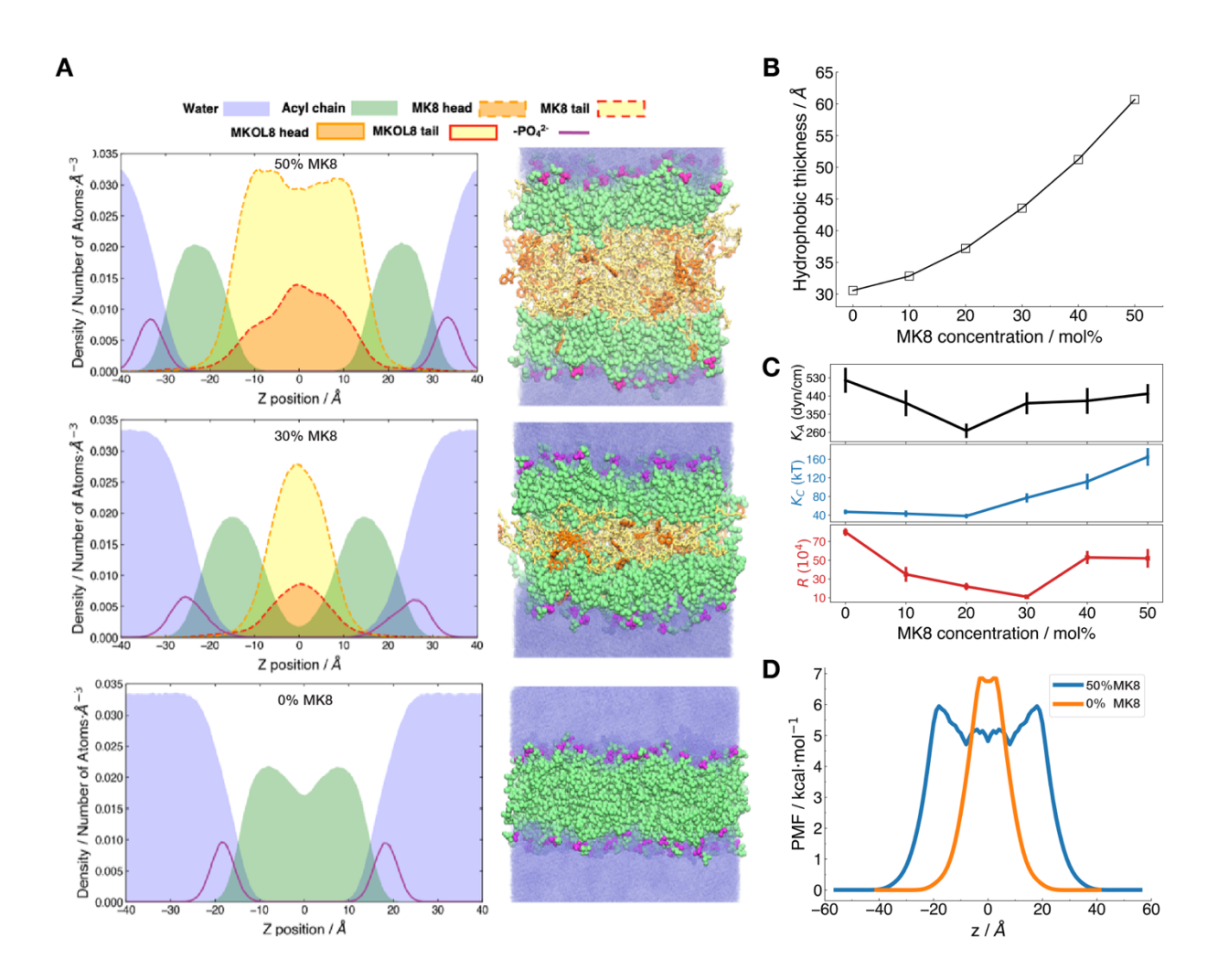


Figure 2. Menaquinone (MK) distributions and its modulation of membrane properties. (A) Distributions of structural elements in 0%, 30%, 50% MK8 systems. Note that MK molecules locate at the membrane midplane (i.e., z=0 along the membrane normal). (B) Membrane bilayer thickness based on central carbon atom of glycerol backbone in the two leaflets increases with MK8 concentrations. (C) Membrane area compressibility modulus (K_A), membrane bending constant (Kc), and water resistance of the membrane with varying concentrations of MK8. (D) Water permeation potential of mean force (PMF) of 0% and 50% MK8. The location of MK8 at the midplane leads to a lowered energy barrier near the midplane. Reproduced from Feng et al.¹⁴ Copyright 2021, American Chemical Society.

We conducted an all-atom MD simulation study to investigate the properties of halobacterial membranes containing varying concentrations (0-50 mol%) of MK8 molecules. ¹⁴ The halobacterial membrane bilayer was modelled with ether-linked phosphoglycerol archaeol (PGAR) and phosphoethanolamine archaeol (PEAR). At the beginning of the simulations, MK8 molecules were placed with their head groups near the water interface and their tails folded like PGAR and PEAR. However, after production simulations, MK8 molecules shift to locate at the membrane midplane regardless of concentrations (10-50%) (**Figure 2A**). As a result, the hydrophobic thickness increases with increasing MK8 concentration in the membrane (**Figure 2B**). This is also corroborated by the fact that the two leaflets are gradually pushed apart with increasing MK8 concentration, and the two leaflets are well separated in the 50% MK8 system with no density of PGAR/PEAR acyl chains in the membrane midplane (**Figure 2A**).

It is of interest to investigate the mechanism of MK8 contributing to hyper-osmotic pressure resistance and establish a rationale for the necessity of 50% MK8. It is known that bacteria keep their outer membrane highly impermeable to detergent and drug molecules. A disruption of the outer membrane lipid packing, for example by antimicrobial peptides or by the appearance of phospholipids instead of lipopolysaccharides in the outer leaflet of the outer membrane, leads to lowered bacterial viability. In order to examine whether halobacteria also employ a tightly packed membrane to block transient water permeation and resist hyper-osmotic pressure, we characterized the membrane rigidity using three approaches. The membrane defect ratio calculates the percentage of hydrophobic core of the membrane exposed to water. The deuterium order parameters (Scd) of the membrane characterize the acyl chain ordering. And the area compressibility modules (K_A) measures the membrane compressibility. None of them yields a significant difference between 0% MK8 and 50% MK8 systems (**Figure 2C**); see also Feng et al¹⁴ for the defect and Scd results.

This finding directed us to the next hypothesis that the condensate might help form a water permeation energy barrier. The potential of mean force (PMF) of water permeation was calculated by $F(z) = -k_BTln(p(z))$, where p(z) is the water probability at a position z along the membrane normal. The PMF of 0% MK8 has a barrier of nearly 7 kcal/mol at the bilayer midplane, similar to bilayers composed of more common phospholipids (**Figure 2D**). In 50% MK8, the free energy plateau in the midplane drops to approximately 5 kcal/mol, as MK8 segregates to the midplane and the barrier associated with the phospholipids tails shifts to approximately z=±9 Å (**Figure 2D**). Therefore, MK is not likely to promote osmotic resistance by increasing permeation barrier. Interestingly, the presence of MK would likely increase the bilayer bending constant Kc, according to the polymer brush model, $K_C = K_A h_{cc}^2/24$, where h_{CC} is the hydrophobic thickness. The K_C is 4 times larger in 50% MK8 system than in 0% MK8 (**Figure 2C**).

The concentration of MK8 is surprisingly high in the halobacterial membrane. We elucidated the localization of such a high concentration of MK8 in the membrane and the potential acting mechanism through increasing bending constant Kc.

3. Ubiquinone partition in a mitochondria inner membrane

Ubiquinone (UQ), a commonly known antioxidant, serves a critical role in the electron transfer chain in mitochondrial membranes. It is a fat soluble lipid consisting of a benzoquinone head and isoprenoid tail of variable lengths in different organisms (**Figure 1**).¹⁵ UQ carries electrons in the electron transfer chain and therefore can switch to its reduced form, ubiquinol (UQOL). Besides its important role in electron transfer chain and ATP synthesis, UQ has been reported to influence membrane properties.¹⁶ Therefore, UQ may possess some biological functions that are still yet to be explored.

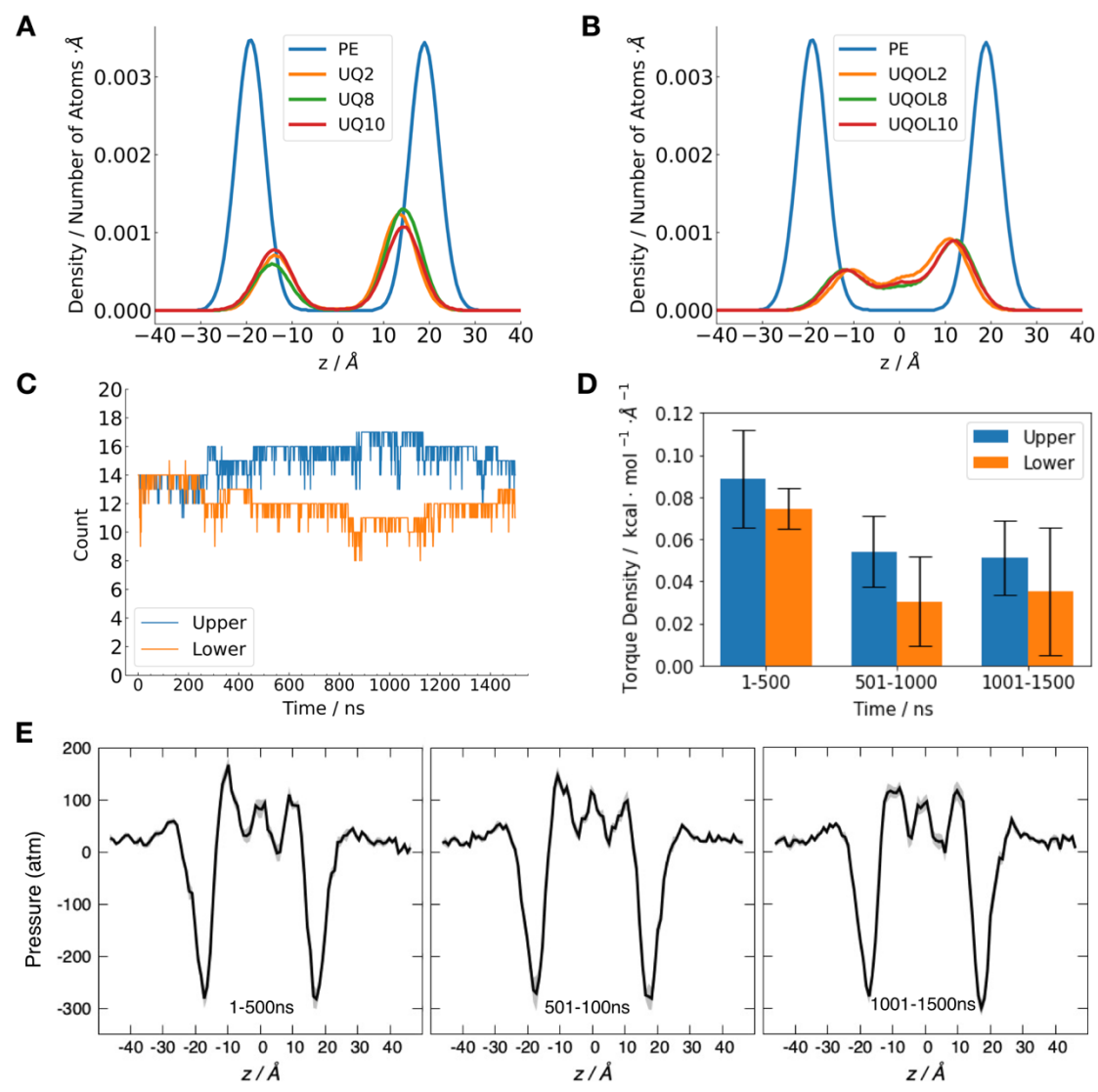


Figure 3. Ubiquinone (UQ) and ubiquinol (UQOL) density profiles, flipflop, and membrane pressure profiles. Headgroup distributions of 5% (A) UQ and (B) UQOL with varying isoprenoid units (2, 8, 10), and of phosphatidylethanolamine (PE) headgroups along the membrane normal. (C) Time evolution of the number count of UQ headgroups in each leaflet of the UQ10 system. (D) Torque density of each leaflet every 500 ns. The error bar represents the standard error calculated with a block size of 5 (i.e., 100 ns). (E) Lateral pressure profile every 500 ns for the

UQ10 system shows the gradual balancing of the pressure profile in the upper and lower leaflets. Grey area shows the standard error with a block size of 5 (i.e., 100 ns).

Previous MD simulation studies used pure or mixed lipid bilayers to explore the localization of UQ. $^{17-19}$ In this study, we built six asymmetric systems in a more complex mitochondrial inner membrane including phosphatidylcholine (PC), phosphatidylethanolamine (PE), and cardiolipin (CL) (see **Table S1** for lipid composition) by adding 5 mol% (28 molecules) UQ or UQOL with tails of 2, 8, 10 isoprenoid units, respectively, using CHARMM-GUI Membrane Builder. $^{20-24}$ The simulation temperature was set to 310.15 K and 0.15 M NaCl ions were included in each system. Each MD simulation was performed for 1.5 μ s (see Supporting Information for simulation details).

The head group distributions along the membrane normal show that UQ has a strong tendency to stay at the membrane-water interface around 15 Å away from the midplane (**Figure 3A**). The majority of UQOL stays with phospholipid acyl chains at around z=±11 Å, but some localize in the membrane midplane (**Figure 3B**). The locations of UQ and UQOL are consistent with experimental data showing that UQOL head group is more immersed in the membrane and the relative headgroup depth in a membrane has no significant dependence on the number of isoprenoid units.²⁵ From a biochemical perspective, it is hypothesized that the location of UQ potentially facilitates reaction in Complex I and Complex III as UQ locates close to the binding sites.¹⁷ The location of UQOL in the midplane may promote electron transfer as it is distributed more uniformly across the membrane.

Interestingly, there is an asymmetric distribution of UQ/UQOL after simulation, with more UQ or UQOL in the upper leaflet (ratio of 1:1,35) (Figures 3A and 3B). UQs flipflop from the lower leaflet to the upper leaflet reaching an equilibrium during the first 500 ns. and then the UQ distribution in each leaflet keeps fluctuating for the rest of the simulation (Figure 3C). This correlates with a decrease in torque density in the first 500 ns, which does not change significantly after that (Figure 3D). Due to the limitation of our simulation time, the standard errors are unsurprisingly high, but we observe an equilibrium in torque density after 500 ns, which matches UQ flipflop equilibrium in the time series. The lateral pressure profile shows the pressure minimum matches the region of polar-nonpolar interface around z=±18 Å, whereas the positive repulsive pressure locates around z=-10 Å and 11 Å for each leaflet, respectively (Figure 3E). The slight difference of the peak location in the two leaflets may be due to the higher concentration of inverted conical lipids such as PE and CL in the inner leaflet. Previous experiment has shown that inverted conical lipids push the lateral pressure closer to the bilayer midplane. ²⁶ The high distribution of PE and CL in the inner leaflet also increases the lateral pressure to the bilayer midplane. Therefore, a pressure gradient exists towards the upper leaflet, which results in UQ/UQOL flipflop and eventually leads to the asymmetric distribution of UQ/UQOL. We also observed a lowered peak in lateral pressure profiles around z=-10 Å and a higher peak around z=11 Å after 1 us (Figure **3E**). Similar function was also found in cholesterol (CHOL), which flipflops to relax surface tension and results in a decrease in the torque density.²⁷ Therefore, the small amount of UQ flipflop may also adjust the lateral pressure.

4. Triacylglyceride lens in ER and pure POPC membranes

Triacylglyceride, or triacylglycerol (TAG), is a neutral lipid consisting of a glycerol headgroup and three fatty acid chains (**Figure 1**). They serve as the main component of animal fat and are a primary energy store for humans. An excess of TAG in the human body, a condition known as hypertriglyceridemia, can be an indicator for weight-related diseases.²⁸ When concentrated in lipid bilayers, TAG molecules display unique properties by forming aggregates in the hydrophobic region. This leads to TAG's significant roles in the genesis and constituency of lipid droplets in

the endoplasmic reticulum (ER).²⁹ Additionally, the formation of these blister-like clusters in membrane bilayers are particularly prominent in malignant cells such as cancer cells.³⁰ Understanding the structure and dynamics of TAG aggregates could provide new insights into the treatment of diseases related to hypertriglyceridemia.

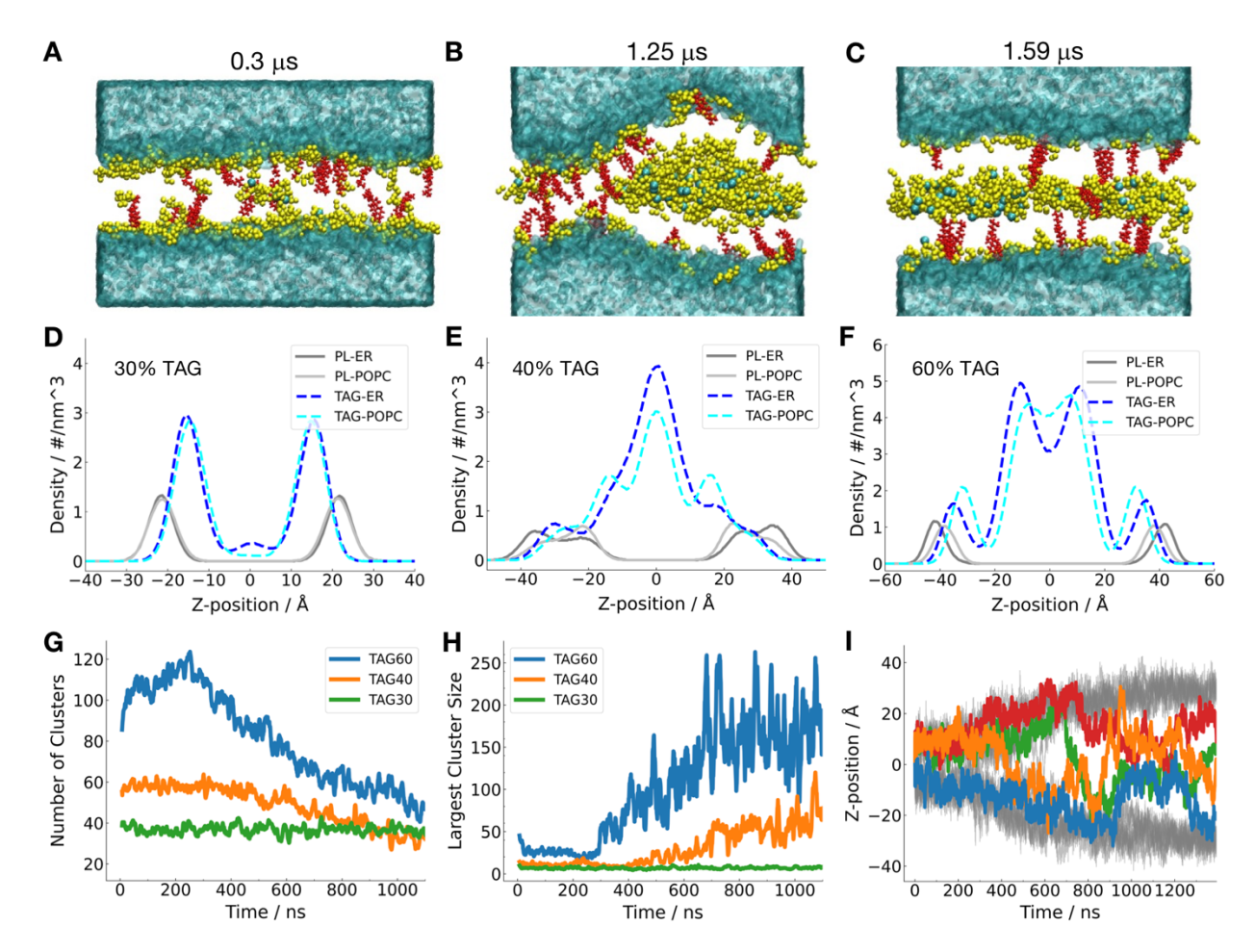


Figure 4. Triacylglyceride (TAG) visualization, density profiles, and clustering analysis of TAG condensates. (A-C) Visualizations of water oxygens (blue), cholesterol (CHOL, red), and TAG headgroups (yellow) in an endoplasmic reticulum (ER) membrane with 40% TAG at 0.3 μs, 1.25 μs, and 1.59 μs. (D-F) Density profiles from 1-1.3 μs of the phospholipid headgroups (phosphorus atoms) and TAG headgroups (oxygen atoms) in the ER membrane and pure POPC membrane with 30% (D), 40% (E), and 60% (F) TAG, respectively. (G-H) Timeseries of the number of clusters (G) and size of the largest cluster (H) in the ER membrane with 30%, 40%, and 60% TAG. (I) Time evolution of CHOL positions along the membrane normal in the 60% TAG-ER system. CHOLs that enter the hydrophobic space with TAG are highlighted in color, while the remaining ones are in gray.

We performed MD simulations to visualize and analyze the aggregation of TAG under different membrane conditions. TAG systems of various concentrations (1-60%) were built with pure POPC or ER lipid composition (**Table S2**)³¹ using CHARMM-GUI Membrane Builder.²⁰⁻²⁴ The simulation temperature was set to 310.15 K and 0.15 M NaCl solution was used. MD simulations were performed for 1.4-3.8 µs for different systems (see Supporting Information for simulation details).

Substantial TAG aggregation starts to appear at 40% or higher TAG concentrations in POPC membranes and at 30% or higher TAG concentrations in ER membranes within 2- μ s simulations. Three phases are generally observed in each of the aggregated systems: (1) descent of small TAG clusters into the hydrophobic region, (2) lens condensation through further aggregation of those small clusters, and (3) the formation of a system-spanning sheet, distinctly separated from the inner and outer leaflets (**Figure 4A-C**). As the TAG concentration was increased, the amount of time required to reach each phase decreased. Additionally, this process occurs faster in ER membranes than in POPC membranes, likely due to POPC membrane being slightly more rigid than ER (i.e., area compressibility modulus (k_A) is 325±55 dyn/cm for POPC and 264±34 dyn/cm for ER).³¹ This is also similar to the finding from tunable coarse-grain simulations that, when membrane rigidity increases, TAG clusters are more planar with high anisotropy.³²

As the TAG percentage increases, pronounced differences in its density profile within a specific timeframe emerge. For 30% TAG, during 1-1.3 µs, the TAG headgroups are symmetrically distributed with most of them locating right below the phospholipid headgroups (**Figure 4D**). In 40% TAG, most of the TAGs have entered the hydrophobic space and formed an asymmetric lens, distorting the leaflets and pushing the phospholipid headgroups away from the hydrophobic region in a minor asymmetric manner (**Figure 4E**). It is evident that the ER system has progressed further in its aggregation than the POPC system with a more pronounced magnitude and normality of TAG distribution. In 60% TAG, the sheet has formed, and symmetry has been restored with the phospholipid heads uniformly pushed approximately 20 Å away from their starting positions (**Figure 4F**). Furthermore, the main aggregate has begun to hollow out in the center along the membrane normal and uniformly widen. **Figures 4A-C** can be viewed as the molecular visualization reflecting the density distributions in **Figures 4D-F**.

To quantify this aggregate process, based on a radial distance function of TAGs (**Figure S1**), a TAG interaction cutoff distance of 10 Å was used. Furthermore, the minimum number of interacting TAG molecules to be considered a cluster was set to 3. In **Figure 4G**, the number of clusters in each system decreases as the small clusters begin to aggregate into a larger cluster. This correlates with the initial increase of largest cluster sizes (**Figure 4H**), which corresponds to the Ostwald ripening phenomenon. In the simulation of 60% TAG in the ER membrane, we also observed that 4 CHOL molecules out of the 20 CHOL pool migrated into the TAG condensate (**Figure 4C and 4I**), indicating that, as TAG extract themselves from the bilayer to form the lens, CHOLs can also be wrapped inside.

5. Perspective discussion

The tugging force between hydrophilicity and hydrophobicity plays a pivotal role in molecular partition in a membrane. For non-bilayer-forming lipids, it is known that charge distributions in headgroups and cross-section area match between the headgroup and acyl chain are important. DAG and TAG both have small, noncharged headgroups and large acyl chain regions, which makes them unable to form a stable bilayer by themselves. For isoprenoids, UQ with a benzene ring has the headgroup located near the lipid-water interface, MK with a naphthalene ring has the headgroup located at the midplane, squalene without a polar head locates at the midplane, while a gemcitabine-squalene conjugate has the large hydrophilic gemcitabine head exposed to water and squalene tail residing in the membrane.³³ This indicates the importance of hydrophilicity of headgroups. Another line of research is on alkanes, which mainly locate at the membrane hydrophobic region.³⁴ From TAG, DAG, to isoprenoids, to alkanes, they constitute a spectrum of neutral hydrophobic compounds that cannot form a bilayer by themselves and the majority of them aggregate at the membrane midplane.

From a force field point of view, Teixeira and Arantes simulated 3 mol% MK9 in a mixed membrane of DLPC and DLPE, and found that MK9 headgroup locates at the lipid-water

interface.¹⁸ Their MK9 parameterization has more polar carbonyl groups and a smaller van der Waals radius for hydrogen atoms than the CHARMM36 FF. Campomanes et al found that the CHARMM36 parameters for TAG and DAG molecules were too hydrophilic at the glycerol-ester region and re-parameterized the charges.³⁵ This agrees with our finding that, with the current CHARMM36, TAG starts to aggregate at a much higher concentration than the ones reported in experiments. Therefore, we note that the non-bonded parameters can impact the simulations results and a careful treatment of the force field parameters will further pave the road of the development in this field.

Besides the localization of the neutral lipids, the next key question is their modulation of membrane properties. This question has practical interest since these molecules can be employed to establish more stable liposomes for drug delivery. UQ has been shown to contribute to membrane rigidity of POPC bilayers and reduce membrane leakage. 16 Squalane is found to contribute to the permeation of large noncharged organic dves, but block the permeation of protons.³⁶ MK, after forming a thick condensate in the membrane, does not alter the membrane rigidity or chain order significantly because it forms a separate phase. One caveat is that the modulation effects have been found to be dependent on lipid types. For example, UQ has a fluidizing effect on POPE membrane, 37 in contrast to its rigidifying effect on POPC, due to the negative curvature of PE lipids. For even more complicated biological membranes such as plasma, ER, and mitochondrial membranes, it would be important to use MD simulations to dissect how the neutral lipids influence the membranes. The CHARMM-GUI website has extensively modelled important biological membrane systems and provide 18 models of these systems (https://www.charmm-qui.org/docs/archive/biomembrane). Currently UQ, MK, TAG, DAG lipids are all available in CHARMM-GUI Membrane Builder. 20-24 We plan to provide the modified DAG/TAG parameters based on Campomanes et al. 35

4 out of 20 CHOL molecules migrate into the TAG lens and stay in the aggregate during the 1.54-μs simulation of 60% TAG-ER system. Though CHOL in the lipid droplet is usually stored in an ester form, a minor amount of free CHOL is also present in the droplet surface.³⁸ CHOL is also shown to influence TAG absorption into the membranes.³⁹ It would be of interest to study the phase behavior and molecular behavior of TAG-CHOL-phospholipid ternary mixtures.³⁰ In such a case, the CHOL concentration in the simulation should be much higher to examine the partition of CHOL into TAG aggregate. Esterified CHOL, cholesteryl esters (CE), has been studied in simulation and found to mainly locate in the lipid droplet core.³⁸ The concept of studying mixtures of neutral lipids in bilayers can also be extended to other molecules such as squalene-MK-archaeal membrane and UQ-CHOL-phospholipids.

The molecular condensates formed by these molecules lead to an increased membrane thickness, but it remains unclear how protein will be impacted by the changes. From our study of 50% MK8 with archaerhodopsin-3, a GPCR protein, the protein stays folded under heightened hydrophobic mismatch tension. The hydrophobic core of α -helix transmembrane proteins is fairly strong regarding unfolding. However, it is not clear how the hydrophobic mismatch might dysfunction membrane proteins such as photocycle of archaerhodopsin, ion conductance and gating of ion channels, and transporting configuration of transporters. For example, squalene accumulation in yeast membranes has been found to be detrimental to cells, though the molecular mechanism underlying such toxicity is unknown. On the other hand, proteins such as seipin assist TAG aggregate formation, the was recently reviewed by Kim et al. Therefore, studying these molecular condensates with key proteins that are associated in biological activities is an ongoing important topic.

An interesting observation from our UQ study in a mitochondrial inner membrane is that UQ flipflops to help release the membrane tension between the upper and lower leaflets. The fact that UQ headgroup is localized in the membrane-water region but the whole lipid is also hydrophobic

enough to flip-flop in the membrane is an interesting property and renders it a membrane tension adjuster. Given the high curvature of cristae in the mitochondria inner membrane, UQ might play a role in adjusting the local membrane pressure. This clearly indicates that a membrane is a dynamic system that uses neutral lipids to constantly release stress in the bilayer.

Research on these neutral lipids can also extend to drug molecules, indicating how they might interact with and modulate the membranes. One important category of drugs are anesthetics. Increasing literature has pointed to their membrane-mediated acting mechanism in addition to direct binding to ion channels. They could disrupt lipid rafts, lower phase transition temperatures, and modulate lateral pressure profiles of lipid bilayers. Another category is probe dyes such as Laurdan. How they behave in a complex membrane containing these neutral lipids is still unknown. The CHOL-TAG aggregate indicates that the neutral lipid aggregate may also absorb probe dyes, interfering with the measurement.

Much of these exciting topics await more studies by various experiments and computational simulations. Adding to the computational modeling arsenal, CHARMM-GUI Membrane Builder currently provides more than 600 lipid types in bacterial, mammalian, yeast, archaea, plant etc., and smoothly connect with all the mainstream simulation software packages. With continuous development and more simulation studies into different neutral lipids in various membranes with/without proteins, our understanding of molecular condensates in the membrane will be much more illuminated.

Supporting Information

Supplementary Tables S1-S4, supplementary Figure S1, and simulation analysis methods.

Acknowledgement

This work was part of the Data4Impact summer undergraduate program at Lehigh University and was supported in part by grants from NSF MCB- 2111728, MCB-1810695, DBI-2011234 (WI).

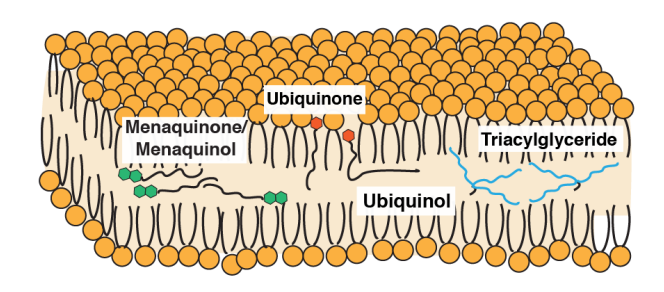
References

- 1. Safinya, C. R., Rädler, J.O., *Handbook of Lipid Membranes: Molecular, Functional, and Materials Aspects (1st ed.).* CRC Press: Boca Raton, 2021.
- 2. Vazdar, M.; Wernersson, E.; Khabiri, M.; Cwiklik, L.; Jurkiewicz, P.; Hof, M.; Mann, E.; Kolusheva, S.; Jelinek, R.; Jungwirth, P., Aggregation of Oligoarginines at Phospholipid Membranes: Molecular Dynamics Simulations, Time-Dependent Fluorescence Shift, and Biomimetic Colorimetric Assays. *The Journal of Physical Chemistry B* **2013**, *117* (39), 11530-11540.
- 3. Gurr, M. I.; James, A. T., Neutral Lipids: glycerides, sterol esters, vitamin A esters, waxes. In *Lipid Biochemistry: An Introduction*, Springer Netherlands: Dordrecht, 1980; pp 90-128.
- 4. LoRicco, J. G.; Salvador-Castell, M.; Demé, B.; Peters, J.; Oger, P. M., Apolar Polyisoprenoids Located in the Midplane of the Bilayer Regulate the Response of an Archaeal-Like Membrane to High Temperature and Pressure. *Frontiers in Chemistry* **2020**, 8.
- 5. Quintero, M.; Cabañas, M. E.; Arús, C., A possible cellular explanation for the NMR-visible mobile lipid (ML) changes in cultured C6 glioma cells with growth. *Biochimica et Biophysica Acta (BBA) Molecular and Cell Biology of Lipids* **2007**, *1771* (1), 31-44.
- 6. Enkavi, G.; Javanainen, M.; Kulig, W.; Róg, T.; Vattulainen, I., Multiscale Simulations of Biological Membranes: The Challenge To Understand Biological Phenomena in a Living Substance. *Chemical Reviews* **2019**, *119* (9), 5607-5774.
- 7. Leonard, A. N.; Wang, E.; Monje-Galvan, V.; Klauda, J. B., Developing and Testing of Lipid Force Fields with Applications to Modeling Cellular Membranes. *Chemical Reviews* **2019**, *119* (9), 6227-6269.
- 8. Venable, R. M.; Brown, F. L. H.; Pastor, R. W., Mechanical properties of lipid bilayers from molecular dynamics simulation. *Chemistry and Physics of Lipids* **2015**, *192*, 60-74.
- 9. Im, W.; Khalid, S., Molecular Simulations of Gram-Negative Bacterial Membranes Come of Age. *Annual Review of Physical Chemistry* **2020**, *71* (1), 171-188.
- 10. Stępień, A.; Koziarska-Rościszewska, M.; Rysz, J.; Stępień, M., Biological Role of Vitamin K— With Particular Emphasis on Cardiovascular and Renal Aspects. *Nutrients* **2022**, *14* (2), 262.
- 11. Kellermann, M. Y.; Yoshinaga, M. Y.; Valentine, R. C.; Wormer, L.; Valentine, D. L., Important roles for membrane lipids in haloarchaeal bioenergetics. *Biochim Biophys Acta* **2016**, *1858* (11), 2940-2956.
- 12. Pumphrey, A. M.; Redfearn, E. R., A method for determining the concentration of ubiquinone in mitochondrial preparations. *Biochemical Journal* **1960**, *76* (1), 61-64.
- 13. Sévin, D. C.; Sauer, U., Ubiquinone accumulation improves osmotic-stress tolerance in Escherichia coli. *Nature Chemical Biology* **2014,** *10* (4), 266-272.
- 14. Feng, S.; Wang, R.; Pastor, R. W.; Klauda, J. B.; Im, W., Location and Conformational Ensemble of Menaquinone and Menaquinol, and Protein–Lipid Modulations in Archaeal Membranes. *The Journal of Physical Chemistry B* **2021**, *125* (18), 4714-4725.
- 15. Meganathan, R., Ubiquinone biosynthesis in microorganisms. *FEMS Microbiology Letters* **2001,** *203* (2), 131-139.
- 16. Agmo Hernandez, V.; Eriksson, E. K.; Edwards, K., Ubiquinone-10 alters mechanical properties and increases stability of phospholipid membranes. *Biochim Biophys Acta* **2015**, *1848* (10 Pt A), 2233-43.
- 17. Galassi, V. V.; Arantes, G. M., Partition, orientation and mobility of ubiquinones in a lipid bilayer. *Biochimica et Biophysica Acta (BBA) Bioenergetics* **2015**, *1847* (12), 1560-1573.

- 18. Teixeira, M. H.; Arantes, G. M., Effects of lipid composition on membrane distribution and permeability of natural quinones. *RSC Advances* **2019**, *9* (29), 16892-16899.
- 19. Kaurola, P.; Sharma, V.; Vonk, A.; Vattulainen, I.; Róg, T., Distribution and dynamics of quinones in the lipid bilayer mimicking the inner membrane of mitochondria. *Biochimica et Biophysica Acta (BBA) Biomembranes* **2016**, *1858* (9), 2116-2122.
- 20. Jo, S.; Kim, T.; Im, W., Automated builder and database of protein/membrane complexes for molecular dynamics simulations. *PLoS One* **2007**, *2* (9), e880.
- 21. Jo, S.; Kim, T.; Iyer, V. G.; Im, W., CHARMM-GUI: a web-based graphical user interface for CHARMM. *J Comput Chem* **2008**, *29* (11), 1859-65.
- 22. Jo, S.; Lim, J. B.; Klauda, J. B.; Im, W., CHARMM-GUI Membrane Builder for mixed bilayers and its application to yeast membranes. *Biophys J* **2009**, *97* (1), 50-8.
- 23. Lee, J.; Cheng, X.; Swails, J. M.; Yeom, M. S.; Eastman, P. K.; Lemkul, J. A.; Wei, S.; Buckner, J.; Jeong, J. C.; Qi, Y.; Jo, S.; Pande, V. S.; Case, D. A.; Brooks, C. L., 3rd; MacKerell, A. D., Jr.; Klauda, J. B.; Im, W., CHARMM-GUI Input Generator for NAMD, GROMACS, AMBER, OpenMM, and CHARMM/OpenMM Simulations Using the CHARMM36 Additive Force Field. *J Chem Theory Comput* **2016**, *12* (1), 405-13.
- 24. Wu, E. L.; Cheng, X.; Jo, S.; Rui, H.; Song, K. C.; Davila-Contreras, E. M.; Qi, Y.; Lee, J.; Monje-Galvan, V.; Venable, R. M.; Klauda, J. B.; Im, W., CHARMM-GUI Membrane Builder toward realistic biological membrane simulations. *J Comput Chem* **2014**, *35* (27), 1997-2004.
- 25. Afri, M.; Ehrenberg, B.; Talmon, Y.; Schmidt, J.; Cohen, Y.; Frimer, A. A., Active oxygen chemistry within the liposomal bilayer: Part III: Locating Vitamin E, ubiquinol and ubiquinone and their derivatives in the lipid bilayer. *Chemistry and Physics of Lipids* **2004**, *131* (1), 107-121.
- 26. H. Templer, R.; J. Castle, S.; Rachael Curran, A.; Rumbles, G.; R. Klug, D., Sensing isothermal changes in the lateral pressure in model membranes using di-pyrenyl phosphatidylcholine. *Faraday Discussions* **1999**, *111* (0), 41-53.
- 27. Miettinen, M. S.; Lipowsky, R., Bilayer Membranes with Frequent Flip-Flops Have Tensionless Leaflets. *Nano Letters* **2019**, *19* (8), 5011-5016.
- 28. Wolska, A.; Lo, L.; Sviridov, D. O.; Pourmousa, M.; Pryor, M.; Ghosh, S. S.; Kakkar, R.; Davidson, M.; Wilson, S.; Pastor, R. W.; Goldberg, I. J.; Basu, D.; Drake, S. K.; Cougnoux, A.; Wu, M. J.; Neher, S. B.; Freeman, L. A.; Tang, J.; Amar, M.; Devalaraja, M.; Remaley, A.
- T., A dual apolipoprotein C-II mimetic-apolipoprotein C-III antagonist peptide lowers plasma triglycerides. *Science Translational Medicine* **2020**, *12* (528), eaaw7905.
- 29. Olzmann, J. A.; Carvalho, P., Dynamics and functions of lipid droplets. *Nature Reviews Molecular Cell Biology* **2019**, *20* (3), 137-155.
- 30. Khandelia, H.; Duelund, L.; Pakkanen, K. I.; Ipsen, J. H., Triglyceride Blisters in Lipid Bilayers: Implications for Lipid Droplet Biogenesis and the Mobile Lipid Signal in Cancer Cell Membranes. *PLOS ONE* **2010**, *5* (9), e12811.
- 31. Pogozheva, I. D.; Armstrong, G. A.; Kong, L.; Hartnagel, T. J.; Carpino, C. A.; Gee, S. E.; Picarello, D. M.; Rubin, A. S.; Lee, J.; Park, S.; Lomize, A. L.; Im, W., Comparative Molecular Dynamics Simulation Studies of Realistic Eukaryotic, Prokaryotic, and Archaeal Membranes. *Journal of Chemical Information and Modeling* **2022**, *62* (4), 1036-1051.
- 32. Kim, S.; Li, C.; Farese, R. V.; Walther, T. C.; Voth, G. A., Key Factors Governing Initial Stages of Lipid Droplet Formation. *The Journal of Physical Chemistry B* **2022**, *126* (2), 453-462.

- 33. Castelli, F.; Sarpietro, M. G.; Micieli, D.; Stella, B.; Rocco, F.; Cattel, L., Enhancement of gemcitabine affinity for biomembranes by conjugation with squalene: Differential scanning calorimetry and Langmuir–Blodgett studies using biomembrane models. *Journal of Colloid and Interface Science* **2007**, *316* (1), 43-52.
- 34. Gruen, D. W.; Haydon, D. A., A mean-field model of the alkane-saturated lipid bilayer above its phase transition. II. Results and comparison with experiment. *Biophysical Journal* **1981**, *33* (2), 167-187.
- 35. Campomanes, P.; Prabhu, J.; Zoni, V.; Vanni, S., Recharging your fats: CHARMM36 parameters for neutral lipids triacylglycerol and diacylglycerol. *Biophysical Reports* **2021**, *1* (2), 100034.
- 36. Salvador-Castell, M.; Brooks, N. J.; Winter, R.; Peters, J.; Oger, P. M., Non-Polar Lipids as Regulators of Membrane Properties in Archaeal Lipid Bilayer Mimics. *International Journal of Molecular Sciences* **2021**, *22* (11), 6087.
- 37. Eriksson, E. K.; Agmo Hernández, V.; Edwards, K., Effect of ubiquinone-10 on the stability of biomimetic membranes of relevance for the inner mitochondrial membrane. *Biochimica et Biophysica Acta (BBA) Biomembranes* **2018**, *1860* (5), 1205-1215.
- 38. Chaban, V. V.; Khandelia, H., Distribution of Neutral Lipids in the Lipid Droplet Core. *The Journal of Physical Chemistry B* **2014**, *118* (38), 11145-11151.
- 39. Spooner, P. J. R.; Small, D. M., Effect of free cholesterol on incorporation of triolein in phospholipid bilayers. *Biochemistry* **1987**, *26* (18), 5820-5825.
- 40. Csáky, Z.; Garaiová, M.; Kodedová, M.; Valachovič, M.; Sychrová, H.; Hapala, I., Squalene lipotoxicity in a lipid droplet-less yeast mutant is linked to plasma membrane dysfunction. *Yeast* **2020**, *37* (1), 45-62.
- 41. Prasanna, X.; Salo, V. T.; Li, S.; Ven, K.; Vihinen, H.; Jokitalo, E.; Vattulainen, I.; Ikonen, E., Seipin traps triacylglycerols to facilitate their nanoscale clustering in the endoplasmic reticulum membrane. *PLOS Biology* **2021**, *19* (1), e3000998.
- 42. Kim, S.; Swanson, J. M. J.; Voth, G. A., Computational Studies of Lipid Droplets. *The Journal of Physical Chemistry B* **2022**.
- 43. Grage, S. L.; Culetto, A.; Ulrich, A. S.; Weinschenk, S., Membrane-Mediated Activity of Local Anesthetics. *Molecular Pharmacology* **2021**, *100* (5), 502-512.
- 44. Lee, J.; Patel, D. S.; Ståhle, J.; Park, S.-J.; Kern, N. R.; Kim, S.; Lee, J.; Cheng, X.; Valvano, M. A.; Holst, O.; Knirel, Y. A.; Qi, Y.; Jo, S.; Klauda, J. B.; Widmalm, G.; Im, W., CHARMM-GUI Membrane Builder for Complex Biological Membrane Simulations with Glycolipids and Lipoglycans. *Journal of Chemical Theory and Computation* **2019**, *15* (1), 775-786.

For Table of Contents Only



Biography

Shasha Feng is a Ph.D. candidate in the Biology program at the Department of Biological Sciences, Lehigh University. She earned her B.S. in Biological Sciences from Peking University, China. Her research is focused on membrane-protein interactions, lipid biophysics, ion channel activation mechanism by lipids and other ligands.

Lingyang Kong is an undergraduate student majoring in bioengineering with a pharmaceutical track at Lehigh University. His research interests are membrane dynamics and protein-ligand interactions.

Stephen Gee is an undergraduate student majoring in biocomputational engineering at Lehigh University. His research interests include lipid biophysics, membrane dynamics, and machine learning.

Wonpil Im is a professor of Biological Sciences, Chemistry, Bioengineering, and Computer Science and Engineering at Lehigh University. He received in bachelor's and master's degrees from Hanyang University in Seoul, Korea. He then earned his Ph.D. in Biochemistry from Cornell University. He did his post-doctoral research at the Scripps Research Institute in La Jolla, California. Research in his lab is focused on the applications of theoretical/computational methods to chemical and physical problems in biology and material sciences. In particular, he is interested in modeling and simulations of biological membranes and associated proteins, glycoconjugates, and protein-ligand (drug) interactions. In addition, his lab has been developing CHARMM-GUI for the molecular modeling and simulation community.